

## SENSITIVITY ANALYSIS OF THE PARAMETERS AFFECTING TEMPERATURE AND PRESSURE PROFILES ALONG THE WELLBORE

Babak Moradi<sup>1,2\*</sup>, Mohammed Ayoub<sup>2</sup>, Mahmood Bataee<sup>3</sup>

<sup>1</sup> LEAP Energy, Suite 14.08, Level 14, G Tower, 199, Jalan Tun Razak, 50400, Kuala Lumpur, Malaysia

<sup>2</sup> Petroleum Engineering Department, Universiti Teknologi PETRONAS, Bandar Seri Iskandar, 31750, Tronoh, Perak, Malaysia

<sup>3</sup> Petroleum Engineering Department, Asia Pacific University, Taman Teknologi Malaysia, 57000, Kuala Lumpur, Malaysia

Received July 20, 2018; Accepted October 19, 2018

---

### Abstract

An appropriate injection well completion design requires a knowledge of pressure and temperature profiles along the depth of the well. The results of sensitivity analysis can be used for preliminary design calculations of injection wells to find the optimum injection surface parameters and wellbore completion. In this study, the surface injection parameters and wellbore geometry are varied to examine the sensitivity of the results for various parameters by using the numerical model during water and gas injections. The results revealed that the temperature profile can be calculated for a single phase with a small error in absence of the pressure profile, the error is less than 3 %. It is found that the contribution of the acceleration term is too weak for building pressure and temperature profiles (less than 0.001%). Further, those comparisons of the results showed that except near the critical point, the pressure profile is not sensitive to the wellhead injection temperature (less than 1 %).

**Keywords:** Energy balance; momentum balance; radiation heat transfer; wellbore design.

---

## 1. Introduction

It has been one of the perennial objectives of the oil industry to increase the oil recovery factor for a given reservoir at the minimum possible cost. This goal has led to the development of numerous improved oil recovery (IOR) techniques [1-3]. Gas (methane, CH<sub>4</sub>, and carbon dioxide, CO<sub>2</sub>) and water injections are among the most common IOR methods used in industry. An Injection well is needed to implement those IOR techniques. An appropriate injection well completion design requires a knowledge of pressure and temperature profiles along the depth of the well [4-9]. The results of sensitivity analysis can be used for preliminary design calculations of injection wells to find optimum injection surface parameters and wellbore completion (e.g. diameter of casing). It will further direct us to parameters which can also influence the pressure and temperature profiles.

## 2. Methodology

In this study, the surface injection parameters and wellbore geometry are varied to examine the sensitivity of results for various parameters by using the numerical model developed Moradi *et al.* [6]. Fig. 1 represents flowchart of the calculation procedure of the numerical model. This numerical model has been selected for conducting the comparison due to it considers:

1. Joule Thompson effect in the wellbore.
2. Variable thermodynamic properties and overall heat transfer coefficient along the well depth.
3. Contribution of kinetic term in the energy balance equation.
4. Contribution of friction and acceleration terms in the momentum balance equation.

Sensitivity studies start with a base case that uses the typical wellbore parameters. Table 1 shows input values used for the base case. Then one parameter at a time is changed to discover the corresponding changes of the wellbore behaviour. This work conducts sensitivity analyses to study effects of wellhead injection temperature, wellhead injection pressure, injection mass flow rate, tubing size, overall heat transfer coefficient, radiation heat transfer, and contribution of different parameters for momentum balance and energy balance.

Table 1. Input parameters as the base case

Parameter	Value	Unit
Depth of the well	914.4	m
Deviation of wellbore from horizontal level	90	degree
Diameter of the wellbore	0.384	m
External diameter of the casing	0.128	m
External diameter of the tubing	0.07424	m
Geothermal temperature gradient	0.0364	°C/m
Injection mass flow rate	1.8	kg/s
Injection temperature at the wellhead	25	°C
Injection time	100	Day
Internal diameter of the casing	0.1152	m
Internal diameter of the tubing	0.064	m
Mean temperature of the surface	21.1111	°C
Thermal conductivity of the cement	0.3462	W/(m.°C)
Thermal conductivity of the earth	2.4234	W/(m.°C)
Thermal diffusivity of the earth	0.00372	m <sup>2</sup> /s

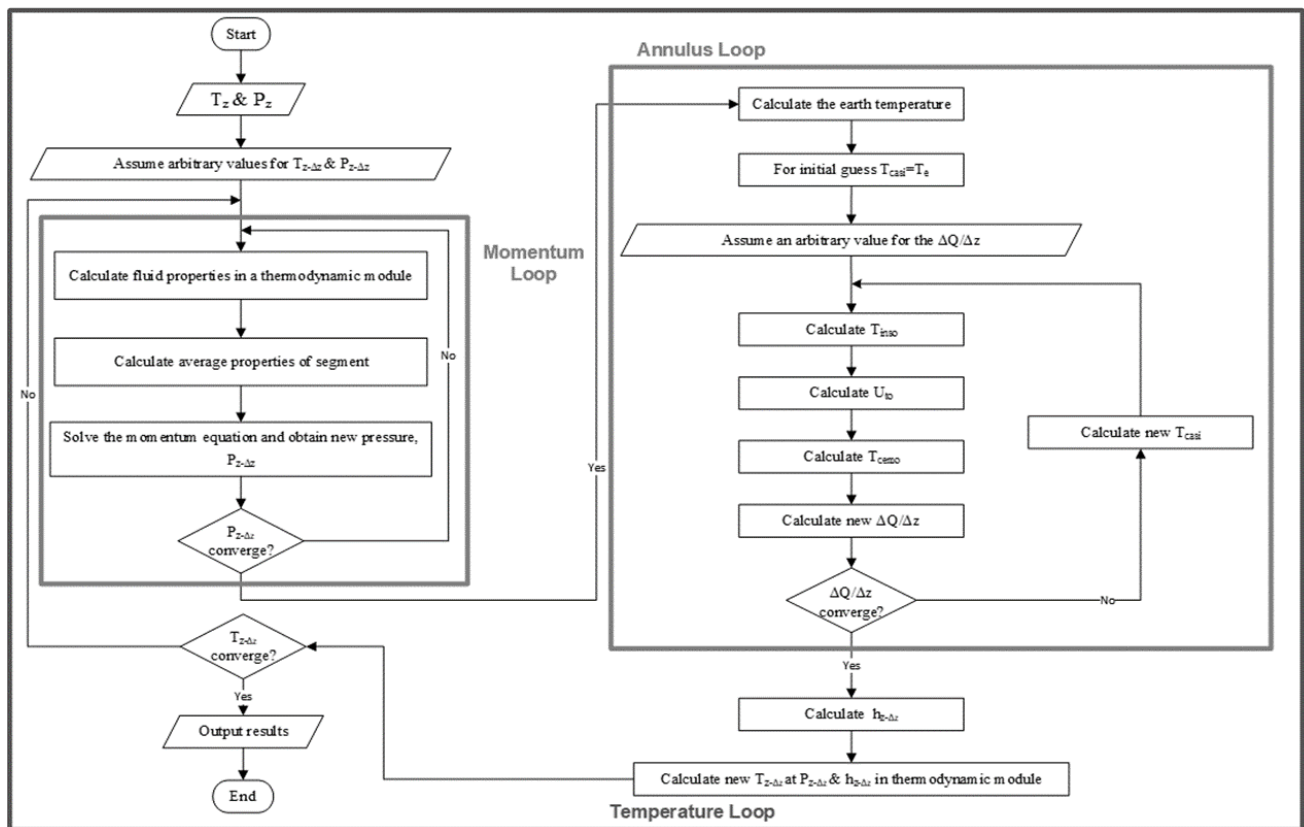


Fig 1. The procedure for calculating the pressure and temperature profiles along the borehole [6]

### 3. Effect of wellhead injection temperature

Fig. 2 represents temperature profiles of the fluid flow in the tubing versus depth at different wellhead injection temperatures (25°C, 65°C, and 105°C) during water, CO<sub>2</sub>, and CH<sub>4</sub> injection processes respectively. Comparisons of the results illustrate that the temperature change of water between the wellhead and bottomhole is less than CO<sub>2</sub> and CH<sub>4</sub>; due to the fact that the heat capacity of water is larger than CO<sub>2</sub> and CH<sub>4</sub> at temperature of 25°C, 65°C, and 105°C [10].

In addition, the results show that the fluid flow temperature inside the tubing during hot fluid injection is much higher than the earth temperature. This fact should be considered during well completion and surface facilities design.

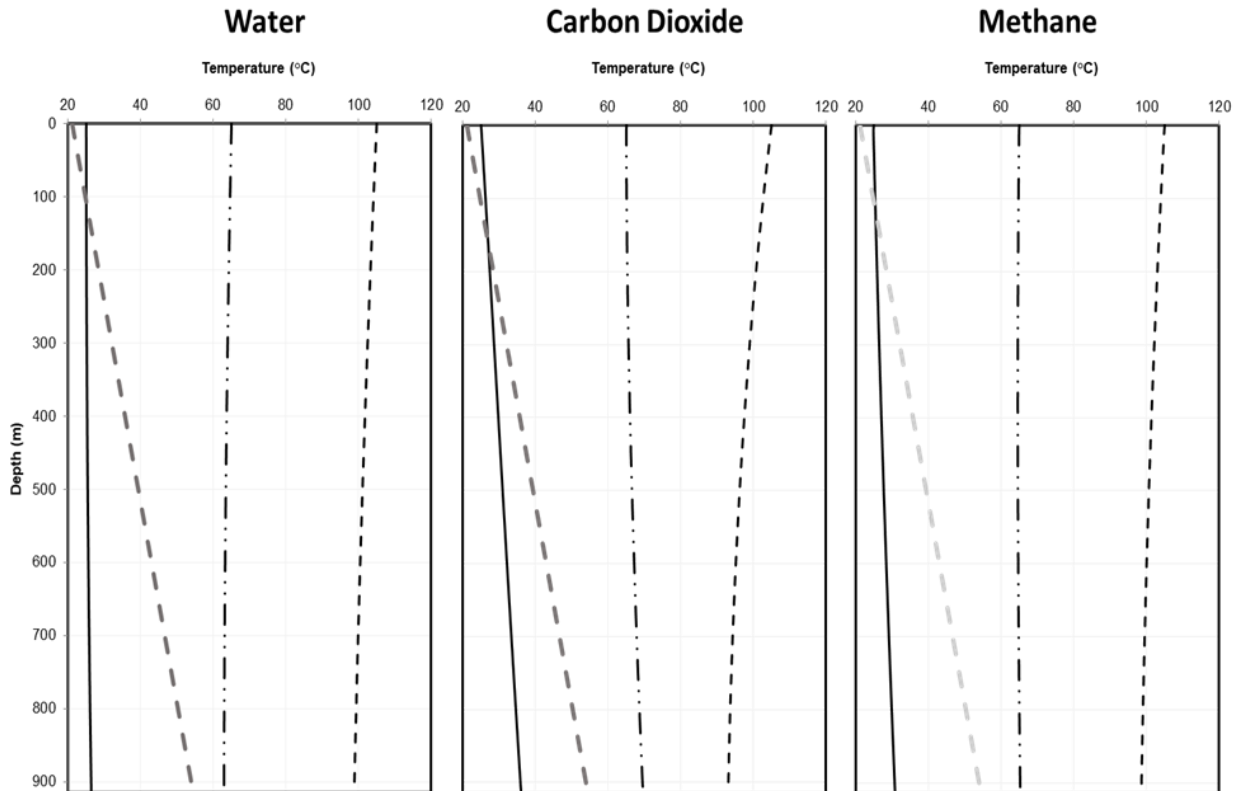


Fig. 2. Temperature profile during water, carbon dioxide, and methane injection at different wellhead injection temperature (—)  $T_{inj}$ : 25 (°C); (-·-·-)  $T_{inj}$ : 65 (°C); (- - - -)  $T_{inj}$ : 105 (°C); (· · · ·) Geothermal temperature

Fig. 3 illustrates pressure profiles of the fluid flow in the tubing versus depth at different wellhead injection temperatures during water, CO<sub>2</sub>, and CH<sub>4</sub> injection processes respectively. Comparisons of the results illustrate that, except near the critical point, the pressure profile is not sensitive to the wellhead injection temperature during water, supercritical CO<sub>2</sub>, and CH<sub>4</sub> injection cases (less than 0.2 MPa), due to the fact that density changes are negligible in a small range of temperature changes at a specific phase. For CO<sub>2</sub> injection case, there is a large temperature profile change between  $T_{inj} = 25^\circ\text{C}$  and  $T_{inj} = 65^\circ\text{C}$  &  $105^\circ\text{C}$  due to phase change. CO<sub>2</sub> exists in liquid phase and near its critical point at  $T_{inj} = 25^\circ\text{C}$  and it is a dense phase at this temperature but CO<sub>2</sub> changes to supercritical phase at  $T = 65^\circ\text{C}$  &  $105^\circ\text{C}$  as it has low density in supercritical condition [11-12], since the build up of the pressure at  $T_{inj} = 25^\circ\text{C}$  is larger than  $T_{inj} = 65^\circ\text{C}$  &  $105^\circ\text{C}$ .

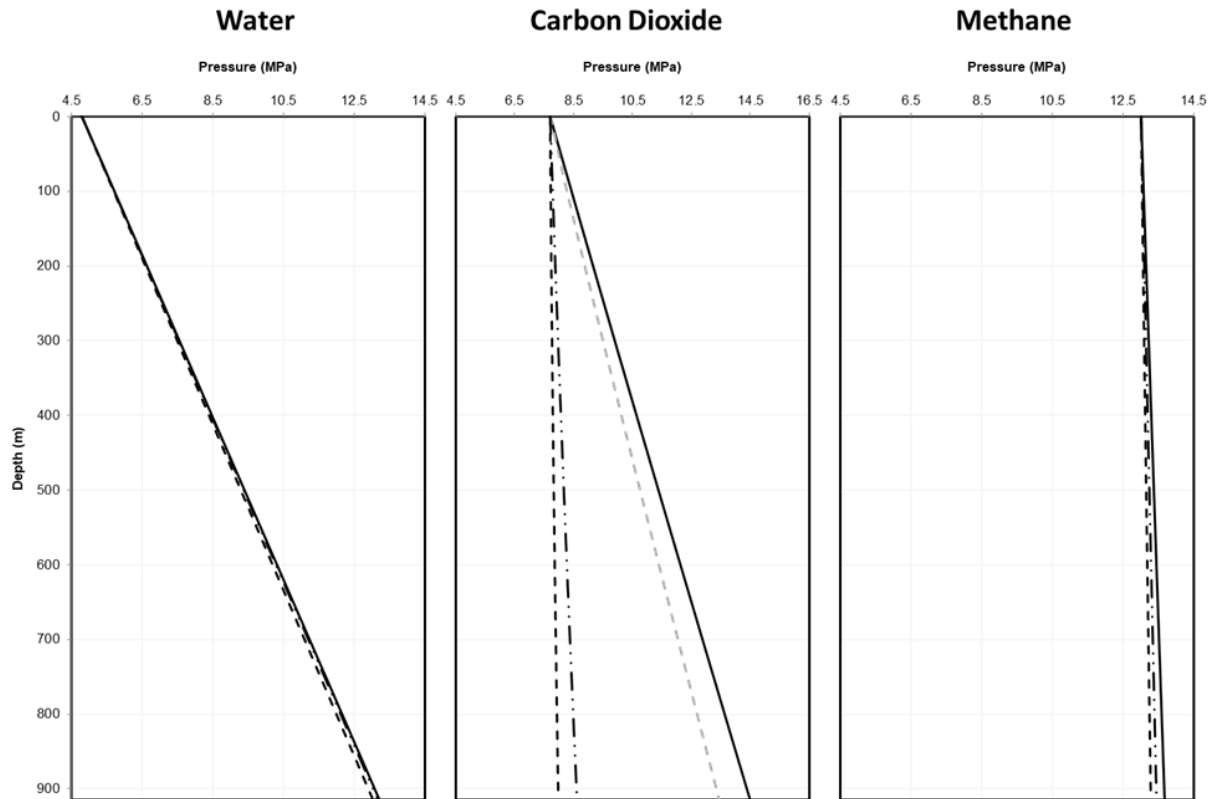


Fig. 3. Pressure profile during water, carbon dioxide, and methane injection at different wellhead injection temperature. (—)  $T_{inj}$ : 25 (°C); (---)  $T_{inj}$ : 31.1 (°C) [Critical temperature of  $CO_2$ ]; (-·-·-)  $T_{inj}$ : 65 (°C); (·····)  $T_{inj}$ : 105 (°C)

#### 4. Effect of wellhead injection pressure

Fig. 4 represents temperature profiles of the fluid flow in the tubing versus depth at different wellhead injection pressures (4.8 MPa and 6.8 MPa) during water,  $CO_2$ , and  $CH_4$  injection processes respectively. Comparisons of the results illustrate that the temperature profile is not sensitive to the wellhead injection pressure and the difference is less than  $1.5^\circ C$ . Fig. 5 shows pressure profiles of the fluid flow in the tubing versus depth at different wellhead injection pressures during water,  $CO_2$ , and  $CH_4$  injection processes respectively. Pressure gradient for water case is larger than  $CO_2$  and  $CH_4$  cases because water has larger density [10-11].

#### 5. Effect of injection mass flow rate

Injection mass flow rate determines the fluid production rate and thus, it is a significant variable [13]. Fig. 6 represents temperatures profiles of the fluid flow in the tubing versus depth at different injection mass flow rates of 0.8, 1.8, 2.8, and 3.8 kg/s for water,  $CO_2$ , and  $CH_4$  injection processes respectively. Comparisons of the results illustrate that temperature differences between the bottomhole and wellhead decreases by increasing the mass injection rate. This is due to the fact higher injection mass flow rate equals higher velocity, therefore the wellbore flow has less time for the heat transfer with the surrounding. The wellbore flow temperature during  $CH_4$  injection case is more sensitive to injection mass flow rate due to its small density and consequently higher velocity.

Injection mass flow rate strongly affects pressure changes during flow as shown in Fig. 9 during water,  $CO_2$ , and  $CH_4$  injection processes respectively. As one would expect, the bottomhole pressure decreases with an increase in injection mass flow rate due to increasing the velocity and subsequently increasing the friction term.

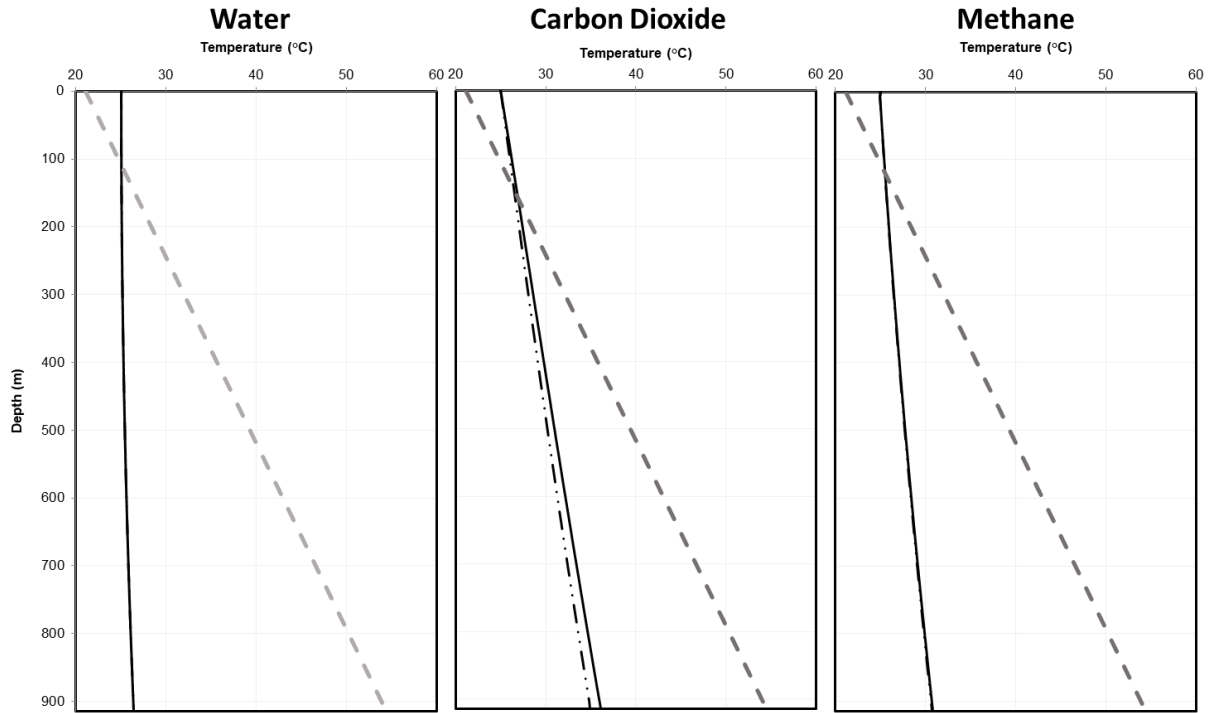


Fig. 4. Temperature profile during water, carbon dioxide, and methane injection at different wellhead injection pressure. (—)  $P_{inj}$ : 4.8 (MPa); (---)  $P_{inj}$ : 6.8 (MPa); (.....) Geothermal temperature

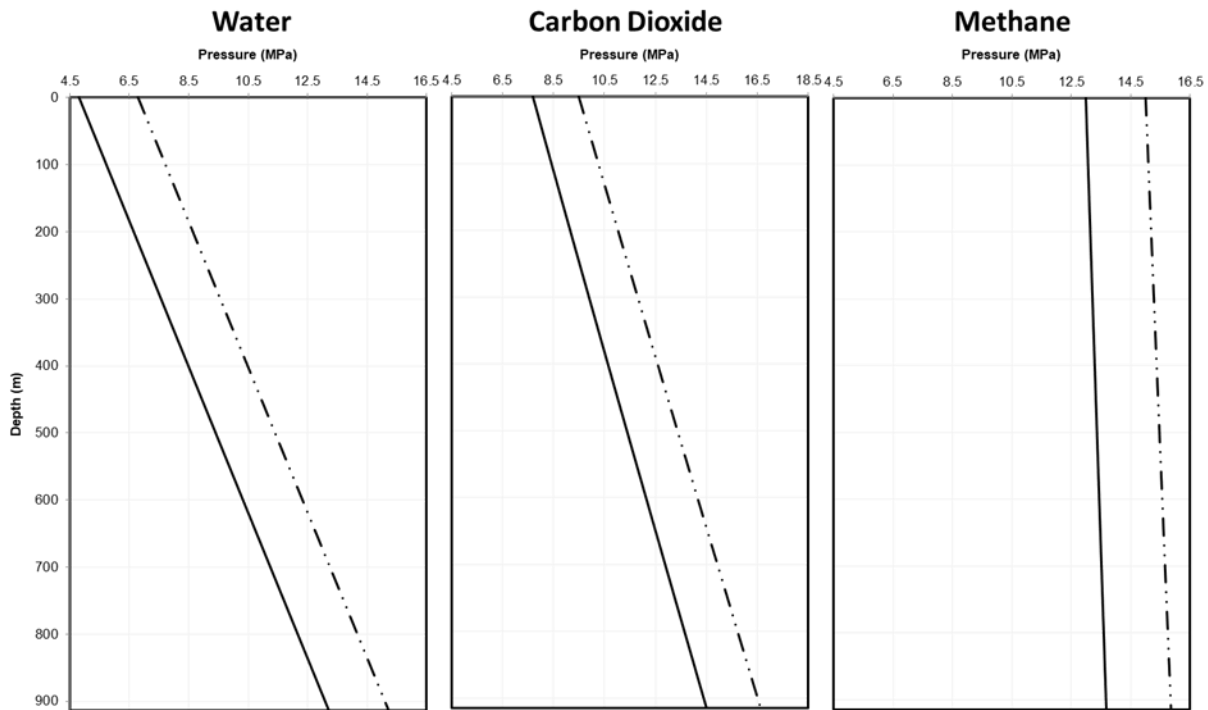


Fig. 5. Pressure profile during water, carbon dioxide, and methane injection at different wellhead injection pressure. (—)  $P_{inj}$ : 4.8 (MPa); (---)  $P_{inj}$ : 6.8 (MPa); (.....) Geothermal temperature

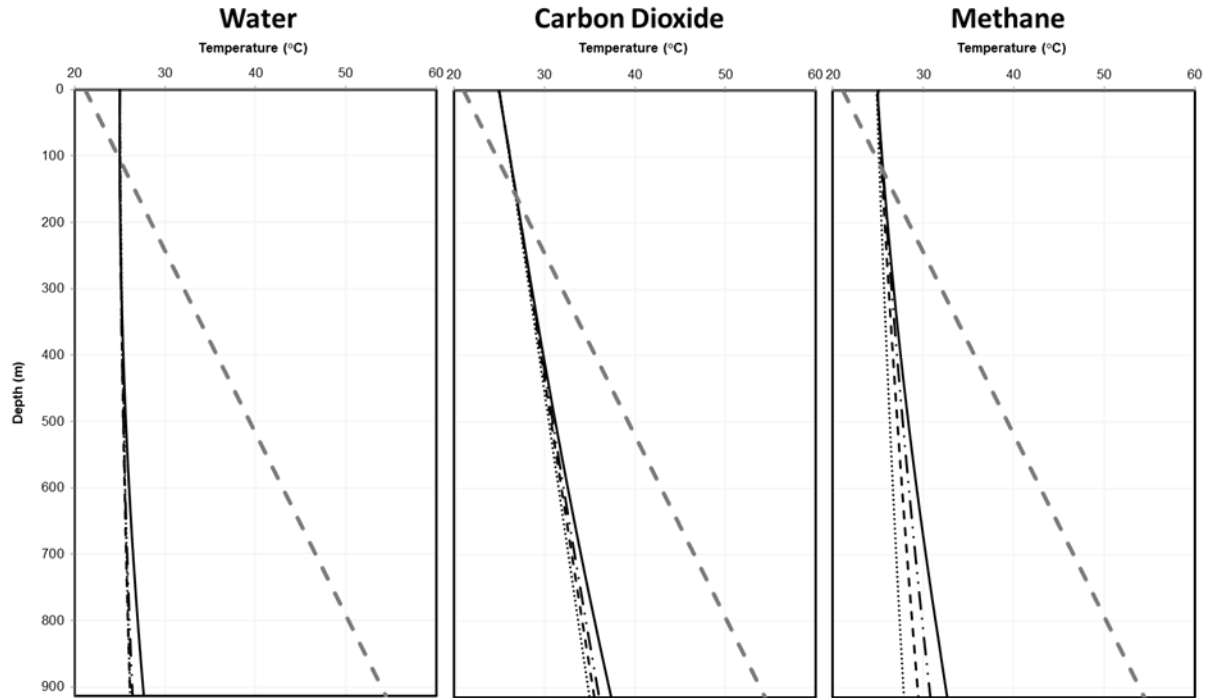


Fig. 6. Temperature profile during water, carbon dioxide, and methane injection at different injection mass rate. (—)  $Mass_{inj}$ : 0.8 (kg/s); (-·-·-)  $Mass_{inj}$ : 1.8 (kg/s); (·-·-·)  $Mass_{inj}$ : 2.8 (kg/s); (·-·-·)  $Mass_{inj}$ : 3.8 (kg/s); (---) Geothermal temperature

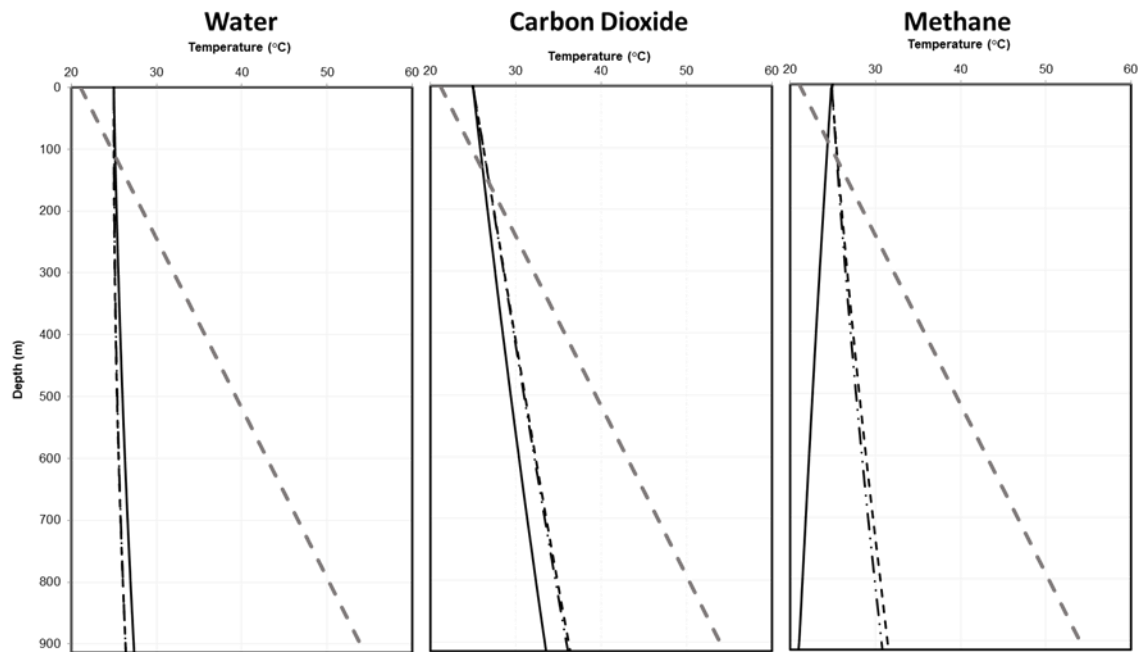


Fig. 7. Temperature profile during water, carbon dioxide, and methane injection at different tubing size. (—)  $R_{tub}$ : 0.01905 (m); (-·-·-)  $R_{tub}$ : 0.03175 (m); (·-·-·)  $R_{tub}$ : 0.0508 (m); (---) Geothermal temperature

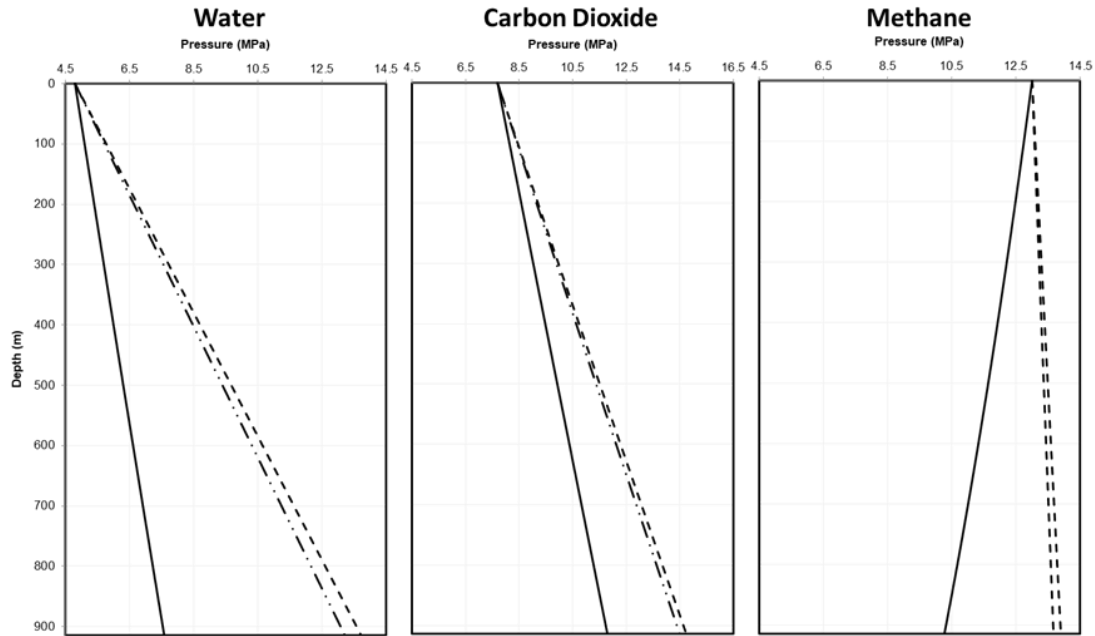


Fig. 8. Pressure profile during water, carbon dioxide, and methane injection at different tubing size. (—)  $R_{tub}$ : 0.01905 (m); (---)  $R_{tub}$ : 0.03175 (m); (.....)  $R_{tub}$ : 0.0508 (m)

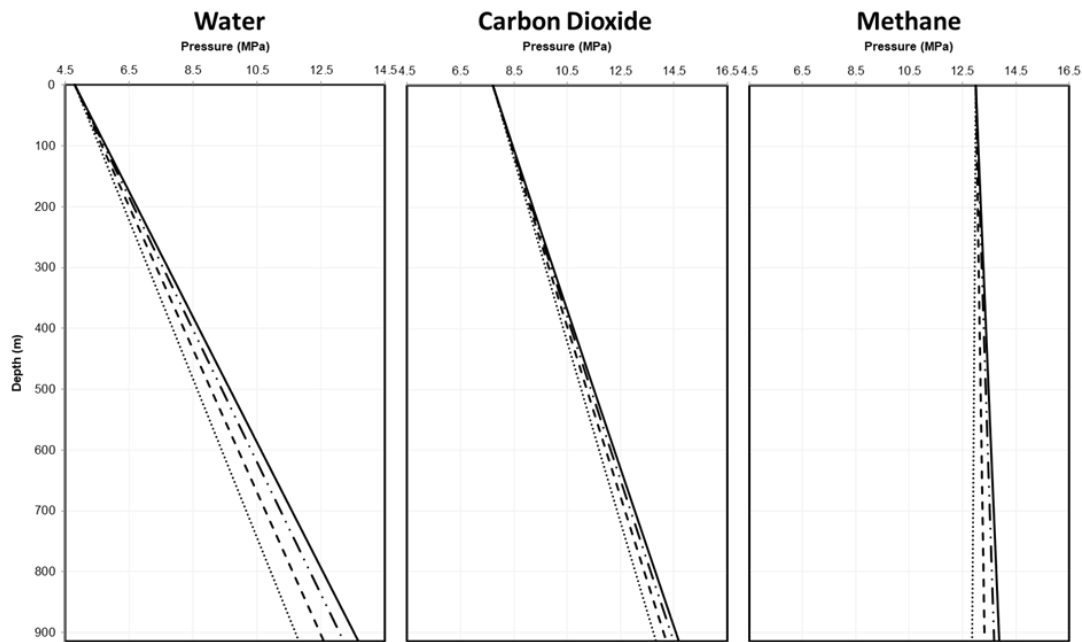


Fig. 9. Pressure profile during water, carbon dioxide, and methane injection at different injection mass rate. (—)  $Mass_{inj}$ : 0.8 (kg/s); (---)  $Mass_{inj}$ : 1.8 (kg/s); (.....)  $Mass_{inj}$ : 2.8 (kg/s); (-·-·-)  $Mass_{inj}$ : 3.8 (kg/s)

### 6. Effect of tubing size

The tubing radii of 0.01905, 0.03175, and 0.508 m were considered in this work to study the effects of the tubing radius on the temperature and pressure profiles. Fig. 7 represents temperature profiles of the fluid flow in the tubing versus depth at different tubing radius sizes

during water, CO<sub>2</sub>, and CH<sub>4</sub> injection processes respectively. Comparison of the results illustrates difference in temperatures between the bottomhole and wellhead decreases by decreasing the tubing radius size. It is because radiation heat transfer between tubing and casing is the predominant heat transfer mechanism for the wellbore and the radiation heat transfer rate is inversely proportional to radii difference of the tubing and casing. Therefore, by decreasing the tubing radius (for a constant casing size), heat transfer rate also decreases. In addition to that, higher fluid flow velocity occurs in the thinner pipe since the wellbore flow has less time for heat transfer with the surrounding in smaller tubing sizes. The wellbore flow temperature during CH<sub>4</sub> injection case is more sensitive to the tubing radius size due to its low density and consequently higher velocity. Fig 8 illustrates pressure profiles of the fluid flow in the tubing versus depth at different tubing radii during water, CO<sub>2</sub>, and CH<sub>4</sub> injection processes respectively. As one would expect, the pressure at the bottomhole decreases with a decrease in the tubing radius due to increasing the velocity and consequently increasing the friction term. There is higher pressure drop for CH<sub>4</sub> injection than water and CO<sub>2</sub> by decreasing the tubing radius because of its low density and consequently higher velocity. The bottomhole pressure decreases more than 5 MPa for a small tubing radius.

### 7. Effect of overall heat transfer coefficient

Overall heat transfer coefficient ( $U_{to}$ ) present thermal conductivity of the wellbore assembly [10]. The thermal resistivity of the wellbore assembly increases by decreasing overall heat transfer coefficient and the heat transfer rate is a linear function of overall heat transfer coefficient [6].

Fig. 10 presents temperature profile of the fluid flow in the tubing versus depth at wellhead injection temperature of 105°C and different overall heat transfer coefficients and injection times during water, CO<sub>2</sub>, and CH<sub>4</sub> injection processes respectively. Comparisons of results for small overall heat transfer coefficient show that the difference of temperature profile in the early and long times is negligible due to lower heat transfer rate between the wellbore flow and wellbore assembly. The difference of bottomhole temperatures are less than 1°C. However, heat transfer rate increases by increasing overall heat transfer coefficient since there is higher temperature drop in long times. Fig. 11 illustrates pressure profile of the fluid flow in the tubing versus depth at wellhead injection temperature of 105°C for different overall heat transfer coefficients and injection times during water, CO<sub>2</sub>, and CH<sub>4</sub> injection processes respectively. Comparisons of the results show that the pressure profile is not sensitive to the overall heat transfer coefficient. The difference in bottomhole pressures is less than 0.4 MPa.

### 8. Effect of radiation heat transfer mechanism

Some commercial software packages [14-15] fail to consider radiation heat transfer mechanism in calculating the wellbore flow temperature. The contribution of the radiation heat transfer mechanism in building the temperature profile is studied in this section. Temperature profile versus depth during water, CO<sub>2</sub>, and CH<sub>4</sub> injection processes at different wellhead injection temperatures with and without consideration of the radiation heat transfer mechanism is presented in Fig. 12. Comparisons of the results show that the consideration of the radiation heat transfer mechanism is not important at low temperature injection (difference in bottomhole temperatures is less than 1°C with and without consideration of the radiation heat transfer mechanism); but by increasing the difference between the wellbore flow temperature and the formation temperature especially during hot fluid injection, it becomes an effective mechanism in heat transfer and it must be considered in temperature profile computations.

Fig. 13 illustrates pressure profiles of the fluid flow in the tubing versus depth at different wellhead injection temperatures during water, CO<sub>2</sub>, and CH<sub>4</sub> injection processes respectively. Comparisons of the results that show the pressure profile is not sensitive to the temperature profile and radiation heat transfer mechanism. The difference of the bottomhole pressures with and with consideration of radiation heat transfer is less than 0.2 MPa.

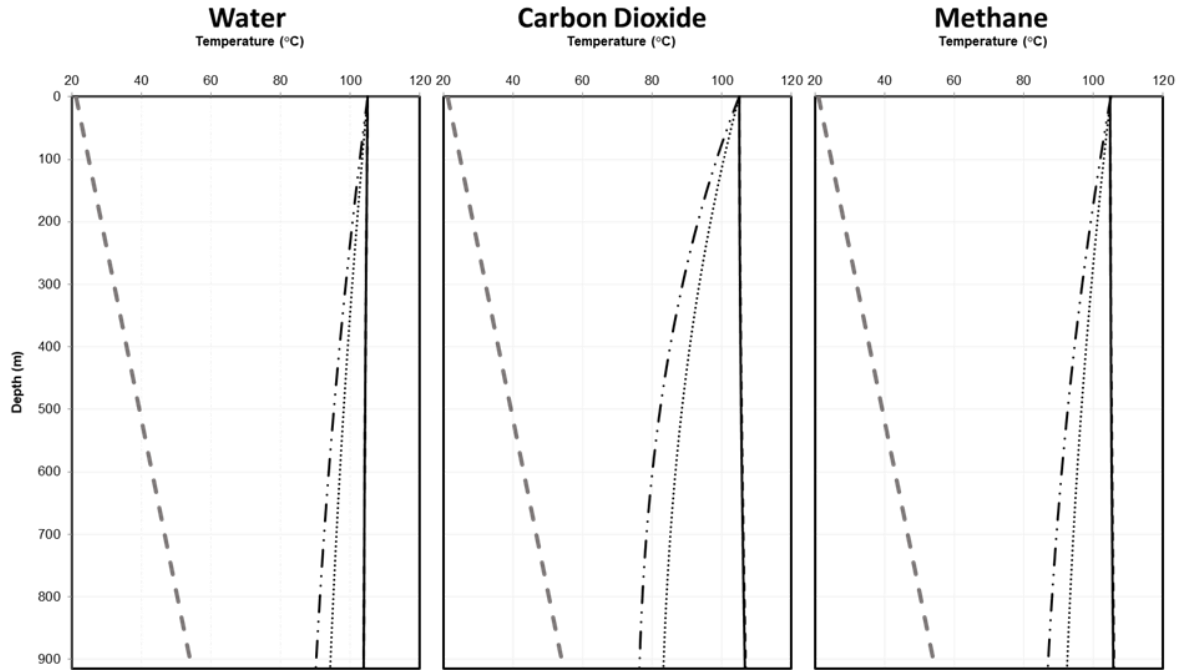


Fig. 10. Temperature profile versus depth during water, carbon dioxide, and methane injection for different overall heat transfer coefficients and injection times at the wellhead injection temperature of 105°C. (—)  $U_{tot}$ : 1 ( $W.m^{-2}.^{\circ}C^{-1}$ ) &  $t$ : 1 (hr); (---)  $U_{tot}$ : 10 ( $W.m^{-2}.^{\circ}C^{-1}$ ) &  $t$ : 1 (hr); (.....)  $U_{tot}$ : 1 ( $W.m^{-2}.^{\circ}C^{-1}$ ) &  $t$ : 2400 (hr); (-.-.-)  $U_{tot}$ : 10 ( $W.m^{-2}.^{\circ}C^{-1}$ ) &  $t$ : 2400 (hr); (.....) Geothermal temperature

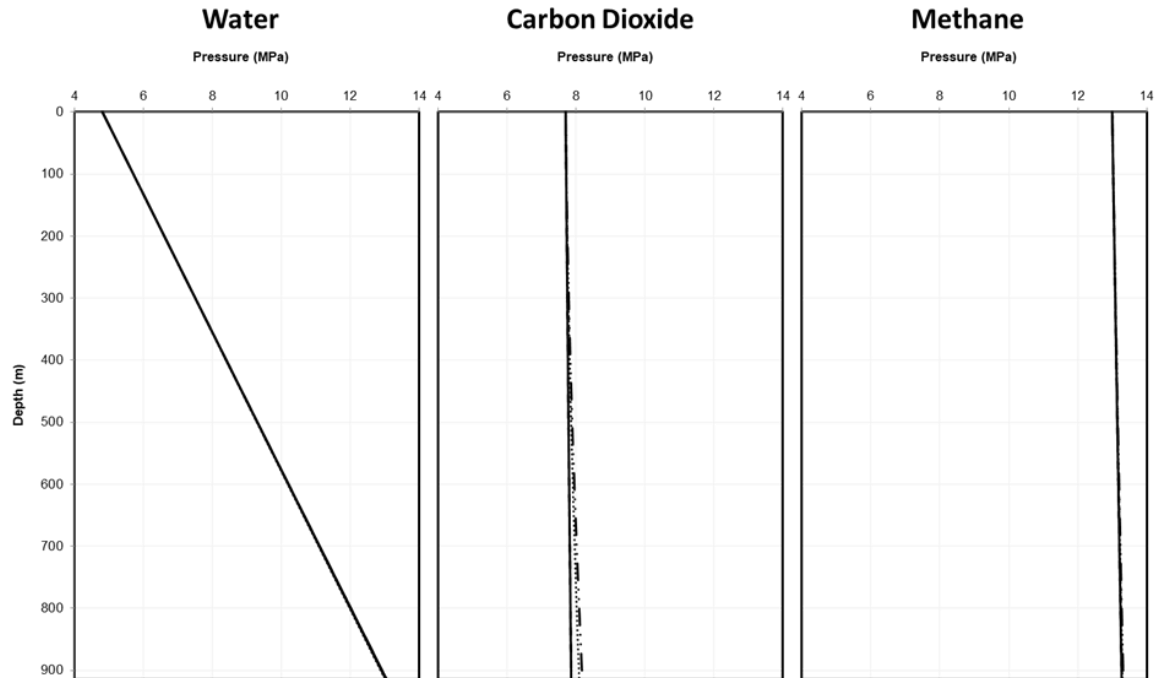


Fig. 11. Pressure profile versus depth during water, carbon dioxide, and methane injection for different overall heat transfer coefficients and injection times at the wellhead injection temperature of 105°C. (—)  $U_{tot}$ : 1 ( $W.m^{-2}.^{\circ}C^{-1}$ ) &  $t$ : 1 (hr); (---)  $U_{tot}$ : 10 ( $W.m^{-2}.^{\circ}C^{-1}$ ) &  $t$ : 1 (hr); (.....)  $U_{tot}$ : 1 ( $W.m^{-2}.^{\circ}C^{-1}$ ) &  $t$ : 2400 (hr); (-.-.-)  $U_{tot}$ : 10 ( $W.m^{-2}.^{\circ}C^{-1}$ ) &  $t$ : 2400 (hr)

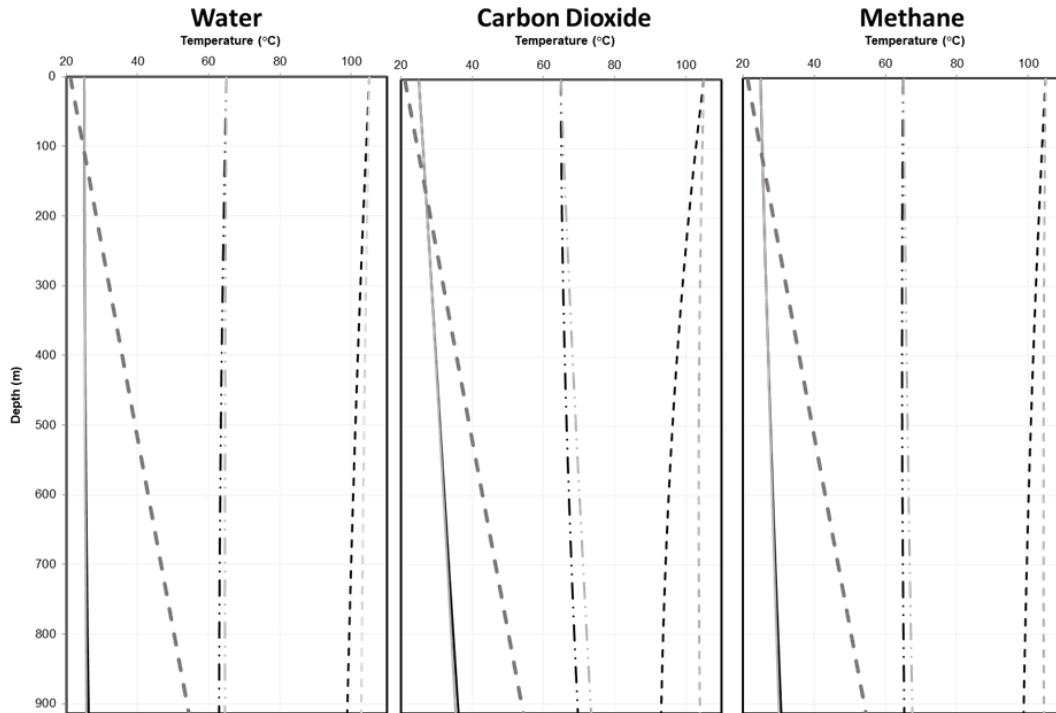


Fig. 12. Effect of the radiation heat transfer mechanism on the temperature profile along the wellbore. (—)  $T_{inj}$ : 25 (°C) [Considered]; (---)  $T_{inj}$ : 25 (°C) [Without consideration]; (-·-·-)  $T_{inj}$ : 65 (°C) [Considered]; (····)  $T_{inj}$ : 65 (°C) [Without consideration]; (- - - -)  $T_{inj}$ : 105 (°C) [Considered] ; (· · · · ·)  $T_{inj}$ : 105 (°C) [Without consideration]; (-·-·-) Geothermal temperature

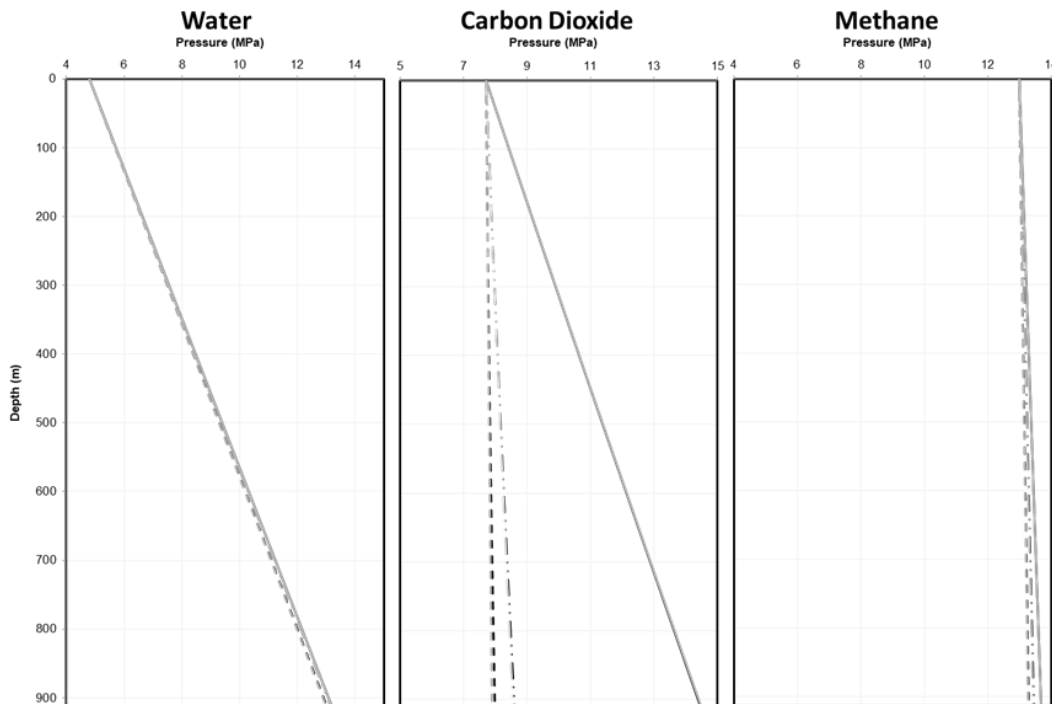


Fig. 13. Effect of the radiation heat transfer mechanism on the pressure profile along the wellbore. (—)  $T_{inj}$ : 25 (°C) [Considered]; (---)  $T_{inj}$ : 25 (°C) [Without consideration]; (-·-·-)  $T_{inj}$ : 65 (°C) [Considered]; (····)  $T_{inj}$ : 65 (°C) [Without consideration]; (- - - -)  $T_{inj}$ : 105 (°C) [Considered] ; (· · · · ·)  $T_{inj}$ : 105 (°C) [Without consideration]

### 9. Effective parameters for momentum balance

The total pressure gradient is the sum of the hydrostatic gradient, acceleration gradient, and frictional gradient [16]. Fig. 14 represents the hydrostatic, acceleration, and frictional terms versus depth respectively. Comparisons of the results [6] show that the contribution of the acceleration term is so weak to build a pressure profile (less than 0.0001 MPa) therefore it can be ignored to conduct faster calculations. The gravity term is the predominant term for building the pressure profile for dense fluid flow (e.g. liquid or near critical point phase) but its contribution reduces in gas phase flow as shown in Fig. 14.

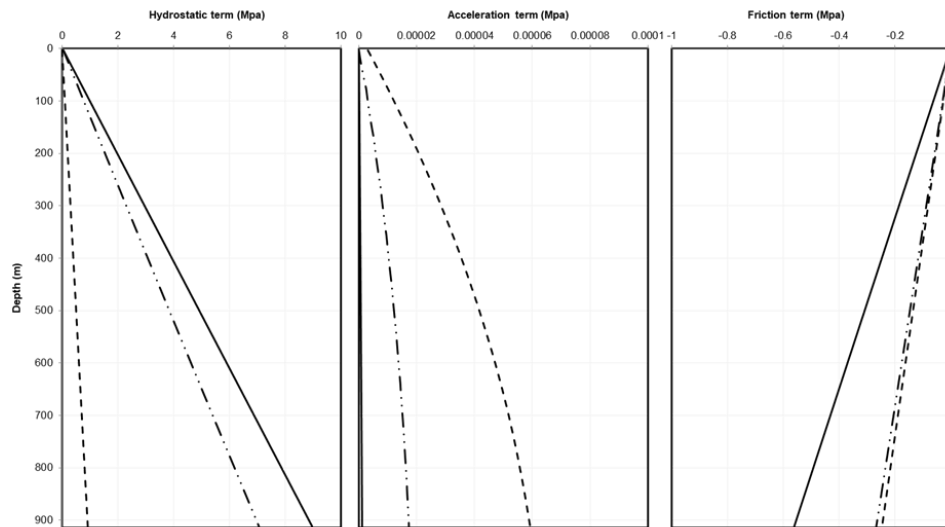


Fig. 14. Contribution of the hydrostatic, acceleration, and friction terms for building the pressure profile. (—) Water; (---) Carbon dioxide; (-----) Methane

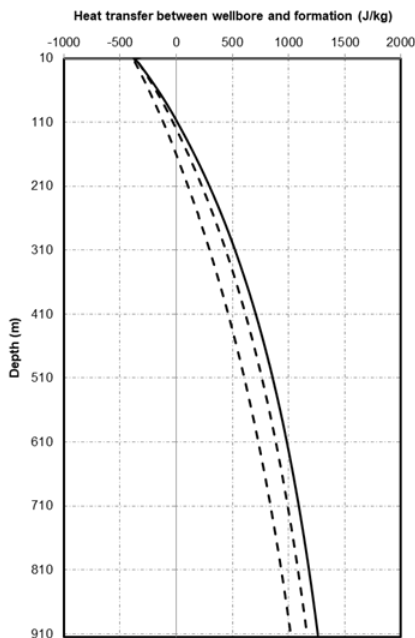


Fig. 15. Contribution of heat transfer between the wellbore and formation term for building temperature profile

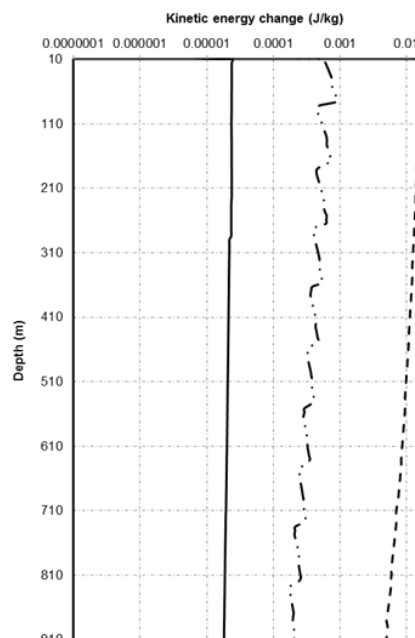


Fig. 16. Contribution of changing the kinetic energy term for building temperature profile

## 10. Effective parameters for energy balance

The energy balance equation includes the change in kinetic energy, potential energy per unit mass, and heat transfer rate between wellbore and formation. The potential energy per unit mass ( $gdz$ ) is constant along the wellbore depth and its contribution depends on the length of the wellbore.

Fig. 15 represents heat transfer at the wellbore/formation interface and Fig 16 shows change in kinetic energy along the wellbore depth calculated by the new procedure. Comparison of Figures 15 & 16 reveals that the kinetic energy change is negligible (less than 0.02 kJ/kg) and therefore, ignoring the kinetic energy term in energy balance equation is a reliable assumption to increase the speed of calculations.

## 11. Conclusions

In this study, the surface injection parameters and wellbore geometry are varied to examine the sensitivity of results for various parameters by using the numerical model developed Moradi *et al.* [6]. The main findings are summarized below:

- During the hot fluid injection, radiation becomes an effective mechanism in heat transfer and it must be considered in temperature profile computations.
- For single phase, the temperature profile can be calculated with a small error in the absence of the pressure profile, (the error is less than 3 %).
- The contribution of acceleration term is so weak for building pressure and temperature profiles (less than 0.001%).
- The pressure profile is a strong function of the tubing size. The bottomhole pressure decreases more than 30 % for a small tubing radius than a large radius.
- Except near the critical point, the pressure profile is not sensitive to the wellhead injection temperature (less than 1 %).

### Nomenclature

$CH_4$	Methane
$CO_2$	Carbon dioxide
$Mass_{inj}$	Injection mass flow rate (kg/s)
$P_{inj}$	Wellhead injection pressure (MPa)
$t$	time (hr)
$T_{inj}$	Wellhead injection temperature ( $^{\circ}C$ )
$U_{tot}$	Overall heat transfer coefficient ( $W.m^{-2}.^{\circ}C^{-1}$ )

### References

- [1] Latil M. Enhanced Oil Recovery. Éditions Technip, 1980.
- [2] Lake LW. Enhanced Oil Recovery. Prentice Hall, 1989.
- [3] Green DW, Willhite GP. Enhanced oil recovery, Society of Petroleum Engineers, 1998. 6th of SPE textbook series.
- [4] Aadnoy BS. Modern Well Design, CRC Press, 2010.
- [5] Leutwyler K. Casing Temperature Studies in Steam Injection Wells, Journal of Petroleum Technology, 1966; 18: 1–157.
- [6] Moradi B, Awang MB, Shoushtari MA. Pressure Drop Prediction in Deep Gas Wells, SPE Asia Pacific Oil and Gas Conference and Exhibition, Jakarta, Indonesia, Society of Petroleum Engineers, 2011.
- [7] Placido JCR, Ademar PJr, Paulo LABF, Pasqualino IP, Estefen SF. Stress-Analysis of Casing String Submitted to Cyclic Steam Injection. Latin American and Caribbean Petroleum Engineering Conference, Rio de Janeiro, Brazil, Society of Petroleum Engineers, 1997.
- [8] Rodriguez-Prada H. Improved Calculation of Casing Strains and Stresses in a Steam Injector Well Simulator. SPE Latin America Petroleum Engineering Conference, Janeiro, Brazil, Society of Petroleum Engineers, 1990.
- [9] Wu J, Gonzalez ME, Hosn NA. Steam-Injection Casing Design. SPE Western Regional Meeting, Irvine, California, Society of Petroleum Engineers, 2005.
- [10] Kreith F, Manglik R, Bohn M. Principles of Heat Transfer. Cengage Learning, 2010.

- [11] Span R, Wagner W. A New Equation of State for Carbon Dioxide Covering the Fluid Region from the Triple-Point Temperature to 1100 K at Pressures up to 800 MPa. *Journal of Physical and Chemical Reference Data*, 1996; 25: 1509–1596.
- [12] National Institute of Standards and Technology, 2011, Available at: <http://webbook.nist.gov/chemistry/fluid/>.
- [13] Ali SMF. A Comprehensive Wellbore Stream/Water Flow Model for Steam Injection and Geothermal Applications. *Society of Petroleum Engineers Journal*, 1981; 21: 527–534.
- [14] Wellflo, 3.6d, Weatherford, 2001.
- [15] VFPi, 2011.2, Schlumberger, 2011.
- [16] Moradi B. A Thermal Study of Fluid Flow Characteristics in Injection Wells. LAP LAMBERT Academic Publishing, 2013.

---

*To whom correspondence should be addressed: Babak Moradi, LEAP Energy, Suite 14.08, Level 14, G Tower, 199, Jalan Tun Razak, 50400, Kuala Lumpur, Malaysia. Email: moradireservoir@gmail.com*